Figure 2. Two-dimensional Fourier transform spectrum (absolute value mode) of the methyl groups in camphor. Note the reversal of the proton and carbon-13 shifts of the *syn*- and *anti*-methyl groups.

mension since the CH coupling provides useful structural information. By recording the two-dimensional spectrum of tetramethylsilane, the frequency axes F_1 and F_2 have been calibrated (in parts per million) with TMS as origin. This new method of shift correlation emphasizes the importance of using a common reference material for protons and carbon-13.

We concentrate on correlating the shifts of methyl groups, since they give the clearest two-dimensional spectra, probably because of a general tendency to be only weakly coupled. Figure 1 shows the methyl region of the spectrum of menthone. Along the right-hand margin of this diagram, in the F_2 dimension, runs the spectrum of three strong decoupled lines from the unmodulated carbon-13 signals; they identify the carbon-13 shifts of sites, a, b, and c, but have no significance for correlation purposes. At each of these F_2 frequencies there is a proton spectrum running in the F_1 dimension, arising from carbon-13 signals that are modulated as a function of t_1. Each such proton spectrum is basically a doublet due to the direct CH coupling, with proton–proton fine structure. This may well be one of the simplest ways of obtaining the proton spectrum of carbon-13 bearing molecules unencumbered by the signals from carbon-12 molecules. The mean frequency of the doublet is a good measure of the proton shift. No analysis of the proton fine structure was made, but it may be noted in spectrum c that there is an evident asymmetry attributable to strong proton–proton coupling.

Of particular interest are the responses that appear near the centres of the a and b doublets but are absent from spectrum c. These signals are transmitted through the two long-range couplings J(C–C–CH$_3$) across the *gem*-dimethyl group. Note that the response of proton a is detected at the chemical shift of carbon b, and vice versa. This characteristic pattern may be used as a diagnostic test for geminal methyl groups, although the absence of long-range responses may only mean that the coupling is weak, leading to signal cancellation.

Figure 2 shows a section of the two-dimensional spectrum of camphor, an example of the reversal of the chemical shift effects for protons compared with carbon-13 in the c (syn) and b (anti) methyl groups. It is immediately clear that the low-field proton shift is associated with the high-field carbon-13 shift, as has been established previously by careful selective double-resonance experiments.[11] Weak responses transmitted through the long-range couplings in the *gem*-dimethyl group are indicated by the arrows.

References and Notes

(1) M. Tanabe, T. Hamasaki, D. Thomas, and L. F. Johnson, *J. Am. Chem. Soc.*, **93**, 273 (1971).
(2) R. Freeman and H. D. W. Hill, *J. Chem. Phys.*, **54**, 3367 (1971).
(3) B. Birdsall, N. J. M. Birdsall, and J. Feeney, *J. Chem. Soc., Chem. Commun.*, 316 (1972).
(4) R. R. Ernst, 18th Experimental NMR Conference, Asilomar, Calif., April 1977; Sixth International Symposium on Magnetic Resonance, Banff, Canada, May 1977.
(5) A. A. Maudsley and R. R. Ernst, *Chem. Phys. Lett.*, **50**, 368 (1977).
(6) W. P. Aue, E. Bartholdi, and R. R. Ernst, *J. Chem. Phys.*, **64**, 2229 (1976).
(7) J. Jeener, Ampere International Summer School Basko Polje, Jugoslavia, 1971; Second Experimental NMR Conference, Enschede, Holland, 1975.
(8) G. Bodenhausen and R. Freeman, *J. Magn. Reson.*, in press.
(9) A. A. Maudsley, L. Müller, and R. R. Ernst, *J. Magn. Reson.*, in press.
(10) G. Bodenhausen, R. Freeman, R. Niedermeyer, and D. L. Turner, *J. Magn. Reson.*, **26**, 133 (1977).
(11) E. Lippmaa, T. Pehk, J. Paasivirta, N. Belikova, and A. Platé, *Org. Magn. Reson.*, **2**, 581 (1970).

Geoffrey Bodenhausen, Ray Freeman*
Physical Chemistry Laboratory
South Parks Road, Oxford, England

Interaction of Acetylene and Ethylene with Nickel Atom

Sir:

The interaction of π-bonded molecules such as acetylene and ethylene with zero-valent metals, particularly organometallic complexes, has long been of interest. Such species are involved in a number of important homogeneous reactions including metathesis,[1] cyclization,[2] hydrogenation, and dehydrogenation.[3] In addition, the smaller unsaturated hydrocarbons, ethylene and acetylene in particular, have become very important in the study of heterogeneous organometallic systems. The techniques of flash desorption,[4] UV PES,[5] and LEED[6] have been used extensively in an effort to elucidate the chemisorptive bonding of unsaturated molecules to metal surfaces.

To gain some detailed understanding of the electronic structure of such species, we have carried out ab initio theoretical studies of π-coordinate Ni-acetylene and Ni-ethylene complexes. The importance of such complexes as simple models for heterogeneous and homogeneous reaction systems has recently been emphasized by matrix isolation studies showing strong similarities in the properties of zero-valent monoolefin complexes and their respective chemisorbed counterparts.[7] Accordingly, we have calculated the optimum geometry of each complex, including electron-correlation effects (generalized valence bond and configuration interaction) and characterized qualitatively the low-lying states.[8]

The results of the geometric optimization are presented in Figure 1. We find that the geometries change only slightly from those of the free molecules. In both cases the CC bond length increases by ~0.02 Å. For acetylene the HCC bond angle is distorted by 5°, while for ethylene the H$_2$C group is distorted by 2°.

The calculated Ni–C bond distances of 2.01 and 2.07 Å for acetylene and ethylene, respectively, are somewhat larger than the values for Ni–C covalent bonds (1.78 Å for NiCH$_2$[9] and 1.87 Å for NiCH$_3$[9]) or σ lone-pair coordination bonds (1.90 Å for NiCO[10]). Although comparison with known organometallic complexes must be made with caution due to the other ligands present in these systems, the results appear to be consistent with the limited structural data available (e.g., [(C$_2$H$_4$)NiP(c-C$_6$H$_{11}$)$_2$]$_2$ shows R(CC) = 1.39 Å and R(NiC)
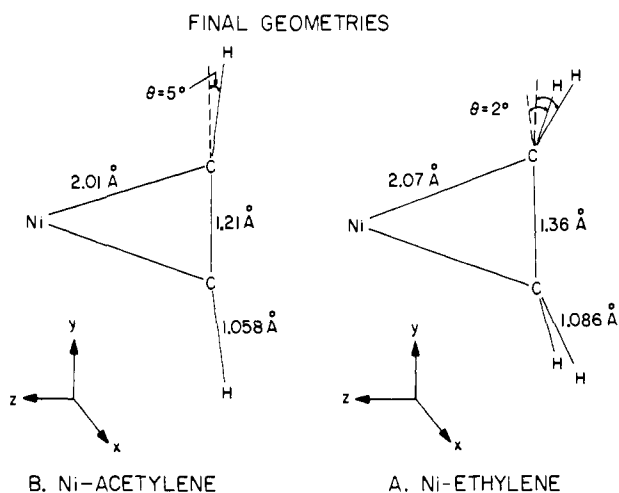
FINAL GEOMETRIES

B. Ni–ACETYLENE   A. Ni–ETHYLENE

Figure 1. Results of geometry optimization from GVB-CI calculations. CH bond distances were fixed at free molecules values.

$= 1.97 \text{ Å}^{11}$). The small distortions found here are in agreement with the interpretation of the UV PES data for these molecules chemisorbed on Ni surfaces (these studies do not provide geometric parameters directly). Similarly, the matrix isolation studies of Ni–ethylene indicate little distortion of the olefin.

The orbitals important in bonding of the Ni-acetylene and Ni–ethylene complexes are shown in Figure 2. Here we find a slight delocation of the π bond (in the NiCC plane) onto the Ni and a slight delocalization of the $d\pi_{yz}$ orbital into the π^* orbital of the ligand. However, these delocalization effects are quite small (certainly smaller than that envisioned in the Dewar–Chatt–Duncansen model[12]), and we view the origin of the bond as follows. Bringing the π bond of the ligand up to Ni^+ ($3d^9$) leads to a significant bond ($\sim$60 kcal) owing to the net attraction of the Ni center for the unshielded π pair. For neutral Ni, the electronic configuration is effectively Ni ($4s^1 3d^9$) with the 4s-like orbital hybridized ($4s$-$4p_z$) behind the Ni to decrease overlap with the ligand orbitals (a Pauli principle effect). This results in a partially unshielded Ni atom that interacts with the ligand much as does Ni^+. The bond energy for the neutral is smaller owing to the repulsive interactions with the 4s orbital. This slight delocalization of the π bond toward the Ni center weakens the π bond, partially accounting for the increased CC bond distance. The slight rehybridization of the π- and σ-bonding orbitals leads to distortion of the CH bonds.

For each of these systems, the lowest electronic states consist of the five different possible occupations of the $3d^9$ shell (triplet coupled to the 4s orbital), in each case spanning a range of $\sim$0.5 eV. The ultraviolet–visible spectrum has been recorded for Ni–ethylene and is dominated by an intense broad band $\sim$280 nm.[7] Preliminary calculations indicate that a strong transition occurs in this region which is a mixture of Ni ($3d_{a_1}$) $\rightarrow$ $4p_y$ and Ni ($3d_{a_1}$) $\rightarrow$ C_2H_4 (π_z^*).

The calculated bond energies are 16.7 kcal/mol for Ni-acetylene and 14.2 kcal/mol for Ni–ethylene. (Both complexes are bound at the Hartree–Fock level of calculation as well; however, the orbital description is considerably different.) We know of no available data for absolute bond energies; however, the relative difference in bond energy of 2.5 kcal for the two hydrocarbons is consistent with ligand displacement studies.[13] The bonding description found here may not apply to multinickel systems. For binuclear metal complexes and for metal surfaces, there are two new alternatives: (a) the acetylene ligand may make similar π bonds with two metal atoms (di-π or μ bonding) or (b) for either C_2H_2 or C_2H_4 one may convert the bonding π orbital into a pair of σ bonds to two different metal atoms (di-σ bonding). Preliminary calculations indicate
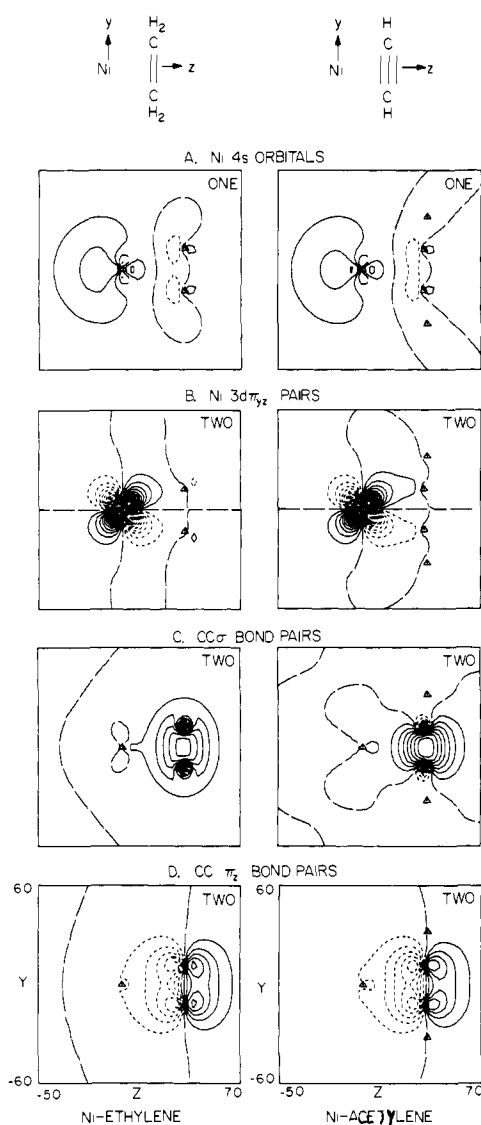

Figure 2. Contour plots of orbitals important in the bonding of Ni–ethylene and Ni–acetylene. Long dashes indicate nodal lines and all contours are uniformly spaced at 0.05 au.

that the transformation from π into di-σ bonding is exothermic by $\sim$23 kcal; however, there may be a significant activation energy for this process (for bonded Ni atoms it is formally a [2s + 2s] cycloaddition and hence Woodward–Hoffmann forbidden).

The results obtained here should apply to other nickel alkene and alkyne systems. The degree to which the ligand distorts, however, will be dependent upon the size (and environment) of the substituents owing to repulsive interactions between the 4s orbital and substituent electron pairs.

In summary, we find that the bonding of Ni to acetylene and to ethylene involves little delocalization of the orbitals, results in small geometric changes, and leads to bond energies of $\sim$15 kcal. These results are consistent with what little experimental data are currently available.

References and Notes

(1) (a) K. G. Caulton, M. G. Thomas, B. A. Sosinsky, and E. L. Muetterties, *Proc. Natl. Acad. Sci. U.S.A.*, **73**, 4274 (1976). (b) For a review, see, for example, N. Calderon, *Acc. Chem. Res.*, **5**, 127 (1972).
(2) W. Reppe, N. von Kutepaw, and A. Magin, *Angew. Chem., Int. Ed. Engl.*, **7**, 727 (1969).

(3) J. M. Manriquez, D. R. McAlister, R. D. Sanner, and J. E. Bercaw, *J. Am. Chem. Soc.*, **98**, 6733 (1976).
(4) J. McCarty, J. Falconer, and R. J. Madix, *J. Catal.*, **30**, 235 (1973).
(5) J. E. Demuth, *Chem. Phys. Lett.*, **45**, 12 (1977).
(6) P. C. Stair and G. A. Somorjai, *J. Chem. Phys.*, **66**, 2036 (1977).
(7) (a) G. A. Ozin, *Acc. Chem. Res.*, **10**, 21 (1977); G. A. Ozin, W. J. Power, T. H. Upton, and W. A. Goddard III, *J. Am. Chem. Soc.*, submitted for publication.
(8) The basis used on the ligand was a full DZ basis of contracted Gaussian functions (T. H. Dunning, Jr., and P. J. Hay in "Modern Theoretical Chemistry: Methods of Electronic Structure Theory", Vol. 3, H. F. Schaefer III, Ed., Plenum Press, New York, N.Y., 1977, pp 1–27) with d polarization functions (α = 0.6769) on the carbons. An effective potential for the Ni atom (C. F. Melius, B. D. Olafson, and W. A. Goddard III, *Chem. Phys. Lett.*, **28**, 457 (1974)) was modified (M. Sollenberger, M. S. Thesis, California Institute of Technology, 1975) to describe correctly the ordering of states in the atom. Using this potential to replace the Ar core of the Ni allowed a truncation of the Ni basis to include only 4s, 4p, and 3d functions (3d contracted DZ for NiC_2H_2, MBS for NiC_2H_4). In the geometry optimization, the CH bond lengths were taken as the free molecule value.
(9) A. K. Rappe and W. A. Goddard III, *J. Am. Chem. Soc.*, **99**, 3966 (1977).
(10) S. P. Walch and W. A. Goddard III, *J. Am. Chem. Soc.*, **98**, 7908 (1976).
(11) B. L. Barnett and C. Kruger, *Cryst. Struct. Commun.*, **2**, 85 (1973). See also C. Kruger and Y. H. Tsay, *J. Organomet. Chem.*, **34**, 387 (1972).
(12) J. Chatt and L. Duncansen, *J. Chem. Soc.*, 2939 (1953).
(13) E. L. Muetterties, private communication.

Thomas H. Upton, William A. Goddard III*

*Contribution No. 5612 from the
Arthur Amos Noyes Laboratory of Chemical Physics
California Institute of Technology
Pasadena, California 91125*

Stereochemistry in the Di-π-methane Rearrangement: Aryl Migration. Exploratory and Mechanistic Organic Photochemistry[1,2]
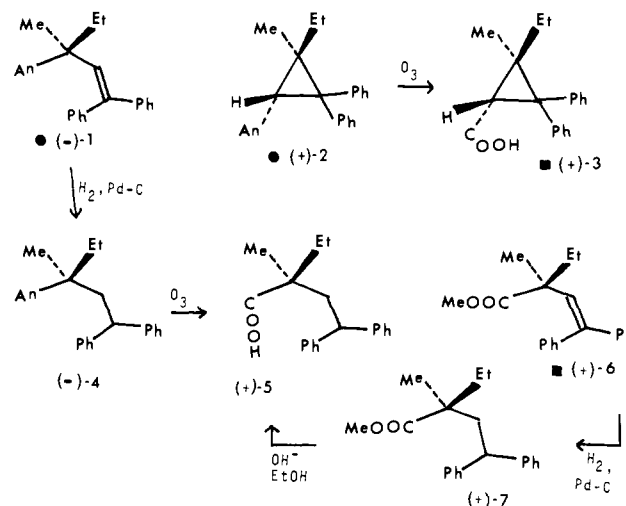
Sir.

There are three known versions of the di-π-methane rearrangement:[3] the divinylmethane variety, the arylvinylmethane type, and the oxa-di-π-methane[3d,e] variation. These differ in many respects. The last generally uses a triplet reactant while examples of the first two involving both singlets and triplets are known. The first two also differ markedly. The divinylmethane rearrangement requires methane carbon substitution while the arylvinyl type does not, the arylvinylmethane singlets tend to react more slowly than their divinyl counterparts,[4] and substituent effects are reversed for these two cases.[4]

The reaction stereochemistry has been studied in only two of the three rearrangements. In our development of the di-π-methane rearrangement,[3a,b,5] we focussed attention on the stereochemistry of the divinylmethane type. At the methane carbon inversion of configuration was found.[5c] In a parallel oxa-di-π-methane example, Dauben[6] has noted almost complete loss of stereochemistry. This is in agreement with the results of Schaffner.[7]

We now report on the stereochemistry of the missing example. Thus we have found complete inversion of configuration at the methane carbon for the arylvinylmethane variation.

For our study we selected 3-p-methoxyphenyl-3-methyl-1,1-diphenyl-1-pentene (**1**), since the central methyl, ethyl substitution was that employed in our previous case[5c] and in the study by Dauben.[6] Also, this reactant and its photoproduct (**2**) could readily be configurationally related to one another using our earlier study[5c] as a basis. The interrelating scheme
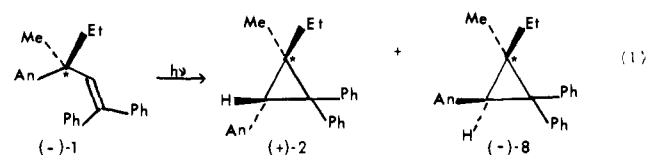
Chart I. Interrelationship of Configurations of Reactant and Di-π-methane Photoproduct[a,b]

[a] Compounds labeled with solid dots are those whose configurations needed to be related. Compounds labeled with solid squares are those whose configurations were known from our earlier study.[5c] [b] Experimentally (−)-**6**, (−)-**7**, and (−)-**5** enantiomers were actually interrelated; reverse configurations are depicted for simplicity of presentation. Optically pure, >99.5%, (−)-**1** was used.

is depicted in Chart I[8] for the trans photoproduct **2**. The cis photoproduct configuration was determined in similar fashion.

Experimentally, direct irradiation of (−)-3-p-methoxyphenyl-3-methyl-1,1-diphenyl-1-pentene (**1**) led to (+)-*trans*-2-ethyl-2-methyl-3,3-diphenyl-p-methoxyphenylcyclopropane (**2**) in addition to the (−)-cis isomer. This allows us to formulate the di-π-methane rearrangement stereochemistry as shown in eq 1.

Inspection of eq 1 reveals that for both diastereomers of photoproduct the configuration at carbon-3 (i.e., the methane carbon) of anisylalkene **1** has been inverted.

Since, even at conversions as low as 15%, 12.8% racemization was observed, there was the question whether the entire reaction mechanism was a concerted one.

However, the low stereospecificity was found to be an experimental artifact rather than real, and our findings indicate how careful one must be in avoiding secondary effects in photochemistry.

Thus, we repeated our irradiations with 10 and 5.6% conversions, and we found diminishing racemization of cyclopropane product with decreasing percent conversion. Owing to overlapping ultraviolet absorption spectra of reactant and product, even at 15% conversion, 4.0% of the light was captured by cyclopropane photoproducts **2** and **8**.

As noted in Table I and Figure 1 extrapolation to zero conversion led almost precisely to zero racemization.

Table I. Optical Purity of Photoproduct **2** vs. Percent Conversion[a]

Percent conversion	14.2 ± 0.7	10.1 ± 0.5	5.6 ± 0.4	Zero conversion[b]
Percent optical purity of photoproduct **2**[c]	87.2 ± 1.5	91.3 ± 1.6	95.0 ± 2.0	100.1 ± 1.7[b]

[a] Measurements at 5 wavelengths, with rotations vs. λ providing evidence of absence of contaminants. [b] Extrapolated value. [c] Each measurement in Table I is the average of two independent determinations.